Langmuir–Blodgett deposition and optical diffraction of two-dimensional opal

Bart van Duffel,[a] Robin H. A. Ras,[a] Frans C. De Schryver[b] and Robert A. Schoonheydt*[a]

[a]Centrum voor Oppervlaktechemie en Katalyse, Katholieke Universiteit Leuven, Kasteelpark Arenberg 23, 3001 Leuven, Belgium. E-mail: Robert.Schoonheydt@agr.kuleuven.ac.be
[b]Afdeling Fotochemie en Spectroscopie, Katholieke Universiteit Leuven, Celestijnenlaan 200F, 3001 Leuven, Belgium

Ammonium-functionalised monodisperse silica spheres have been prepared and spread together with sodium dodecylsulfate at the air–water surface. The resulting particulate films have been deposited on various substrates. The Langmuir isotherm has been used to estimate the density and refractive index of the particles. The films exhibit vivid optical diffraction due to a high degree of ordering of the particles. The lattice constant of this two-dimensional opal structure has been determined by atomic force microscopy at 536 nm. Optical diffraction of the films has been established and explained in terms of a Bragg-like diffraction. The lattice constant, as determined by optical diffraction, is found to be in good agreement with the AFM measurement, within experimental error. We consider this Langmuir–Blodgett deposition of 2D opal as a promising route for the preparation of active layers in photonic band gap devices and materials.

Introduction

Preparation of highly functional materials requires the organisation of different components (organic and biological molecules, polymers, colloids, etc.) from the molecular up to the submicron scale. Langmuir–Blodgett (LB) deposition and self assembly techniques have proven to be valuable methods to achieve such organisation.[1] While self assembly techniques[2–5] are versatile and fast, Langmuir–Blodgett deposition[6–10] generally allows a higher degree of control over the organisation of the system. This advantage has inspired us to explore LB deposition as a tool for the preparation of a new class of optical materials, photonic band gap materials.

Photonic band gap (PBG) materials are dielectric materials ordered at the submicron to micron scale, with high refractive index contrasts.[11–18] These structural characteristics generate the photonic band gap property. For a discrete band of wavelengths, transmission of electromagnetic radiation is completely forbidden. Much like electrons and X-rays interact with the crystalline (ordered) structure of semiconductors at the atomic scale, visible light waves interact with the ordered structure of PBG materials at the submicron scale, hence the band gap properties. The PBG property forms the physical basis for a wide range of fascinating properties and applications, such as enhancement and inhibition of spontaneous emission,[12,15] ultrafast optical switching,[19,20] optical insulation,[20] etc. In a true PBG material, transmission of light is forbidden in all directions and for all polarisations. Although this requires a 3D structure, 2D ordered structures have been demonstrated to exhibit useful PBG properties.[15,17] A promising basic structure for the preparation of PBG materials is synthetic opal.[21–25] Ideally, it consists of an array of monodisperse SiO_2 spheres ordered into a face centred cubic (fcc) packing. The fcc structure can be envisaged as an ABC stacking of layers with a 2D hexagonal close-packing (hcp) of spheres.[26] Usually, synthetic opal is prepared by sedimentation of SiO_2 spheres in a dilute colloidal suspension.[21–25]

Here we explore Langmuir–Blodgett deposition as a method for the preparation of large area 2D synthetic opal as a basis for the preparation of advanced optical materials. This approach can be envisaged as a first step in a controlled, layer-by-layer procedure for the preparation of large area synthetic opal.

Experimental

Preparation of monodisperse hydrophilic SiO_2 beads

Monodisperse silica microspheres were prepared according to Stöber's method.[27,28] Briefly, to 50 ml of a 2 M NH_3–6 M H_2O ethanolic solution were added 8.5×10^{-3} mol of tetraethyl orthosilicate (ACROS, 98%), which was left stirring overnight to polymerise. Then, the suspension was centrifuged at 3000 rpm for about 20 min, the ethanolic supernatant was decanted and the silica was redispersed in 20 ml of deionised water. To this suspension was added dropwise, while stirring, 10 μl of a 50% methanolic solution of [3-(trimethoxysilyl)-propyl]trimethylammonium chloride (Gelest) and the suspension was left to stir for a day. Next, the suspension was washed by centrifugation and redispersed in water. This washing cycle was repeated 3 times. Finally, the resulting beads were dried in a vacuum oven at 60 °C.

Preparation of the silica microsphere suspension

25 mg of the silica beads were suspended in 1.5 ml of a 1.67×10^{-3} M sodium dodecylsulfate (Aldrich, 98%) solution in chloroform/ethanol (80/20 v/v). Prior to spreading, the suspension was ultrasonicated for at least half an hour. The resulting suspension was slightly opaque.

Measurements

Films were prepared and isotherms recorded on a NIMA Technology model 611 Langmuir–Blodgett trough. Milli-Q water was used as the subphase. Atomic force microscopy images were obtained on a Topometrix Discoverer TMX 2010 system with a Si_3N_4 tip in contact mode. The force constant of the cantilever was 0.032 N m^{-1}. Optical diffraction spectra were recorded on a SLM 8000C spectrofluorimeter (SLM instruments Inc.) in a synchronous scan mode. A mirror accessory was built to measure diffraction spectra.

Results and discussion

Langmuir–Blodgett deposition and AFM characterisation of the particulate films

A suspension of the ammonium-modified SiO_2 spheres in a sodium dodecylsulfate (SDS) chloroform/ethanol solution was spread onto the water subphase. The solvent was left to evaporate for 30 min prior to compression of the film. In Fig. 1, a representative isotherm (25 °C) of the particle film is presented. The slope of the isotherm is extremely steep, indicating a very low compressibility. Beyond surface pressures of $15 \, mN \, m^{-1}$ the film becomes slightly opaque, which indicates the first collapse. This is much before the collapse is apparent from the isotherm (beyond $20 \, mN \, m^{-1}$). In the absence of SDS, no films could be prepared. The films can be easily deposited at $\Pi = 5 \, mN \, m^{-1}$ in upstroke onto various substrates, such as glass and Si-wafer. On all substrates, the films exhibit vivid colours. The structure of the films was imaged using AFM in contact mode. It reveals a long range ordering of the SiO_2 spheres. As can be seen from Fig. 2, the spheres are ordered into a hexagonal close-packed monolayer. The films show some ordering defects, the most common being the presence of vacancies (arrow 1) and local cubic ordering of the spheres ('zipper') (arrow 2). The sphere-to-sphere (periodic) distance was determined to be 536 nm ($\sigma = 39.5$ nm). This value includes lattice disorders. If the lattice disorders are not taken into account, we obtain a value of 528 nm for the sphere-to-sphere distance, which is also the average particle diameter.

The film density, δ_{Film}, is defined as mass [of particle(s)] per unit area (g nm^{-2}):

$$\delta_{Film} = \frac{m}{S} \qquad (1)$$

The unit cell of the hcp structure is shown in the top right corner of Fig. 2. The unit cell contains the total mass of one sphere, m, where $m = \frac{4}{3}\pi r^3 \delta_{sph}$, with δ_{sph} the density of the silica spheres and r their radius. The total area, S, of the unit cell is equal to $2\sqrt{3}(r^2)$. Assuming perfect hexagonal close packing, δ_{Film} of the unit cell equals δ_{Film} of the whole film. Thus, the expression for the film density becomes:

$$\delta_{Film} = \frac{m}{S} = 1.209 \delta_{sph} r \qquad (2)$$

With equation (2), the density of the spheres δ_{sph} can be estimated from the Langmuir isotherm if the amount of particles spread (m) and the particle size (determined by AFM at 528 nm) is known. In analogy with molecular films, we assume that the surface is covered by densely packed particles at the zero-pressure "molecular" area.
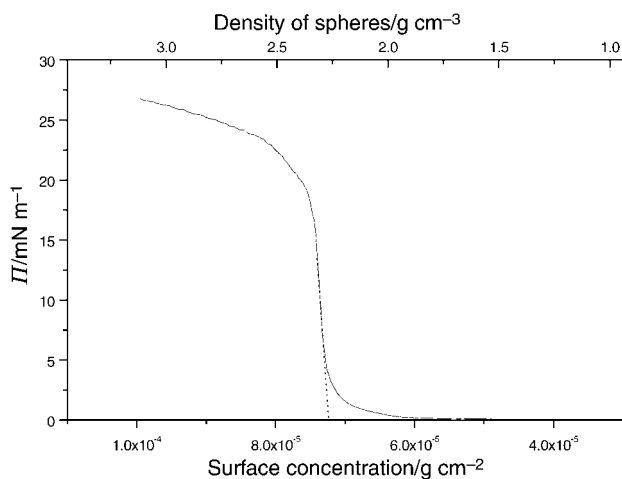

Fig. 1 Langmuir isotherm of ammonium-modified silica spheres spread together with SDS. The upper abcissa shows the density of the spheres.
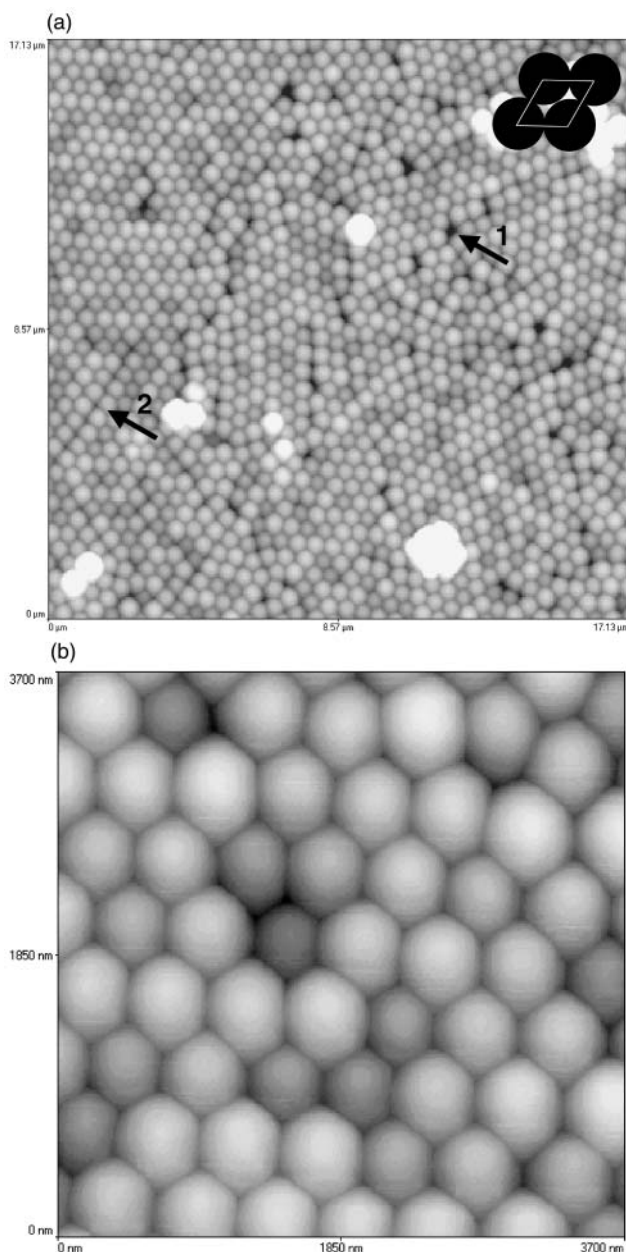

Fig. 2 AFM topographical images of the Langmuir–Blodgett film of SiO_2 spheres. (a) Large-scale scan (17.1 μm) showing some defects (indicated by arrows) in the film structure, as well as some spheres lying on top of the film. The unit cell of the hcp structure is depicted in the inset. (b) Small-scale image (3700 nm) showing the hcp structure of the film. As this is a topographical image, the darker the particles the smaller their size.

The density of the particles is indicated on the upper abcissa in Fig. 1. The estimated value for δ_{sph} is about $2.25 \, g \, cm^{-3}$. Taking the imperfect hcp structure and the experimental error into account, this value is comparable to the density of fused SiO_2 ($2.2 \, g \, cm^{-3}$).[30] Stöber spheres in general, however, are known to have some porosity, even though porosity decreases with particle size.[33] It is likely that the micropores of the particles are still filled with water, as they were only dried at 60 °C. This results in higher particle densities compared to those of fully calcined silica spheres. In addition, the present method has some experimental error which needs to be further established.

The refractive index of the spheres can be estimated using a simple averaging approach. Thus, $n_{sph} = n_{SiO_2} V_{SiO_2} + n_{void} V_{void}$, where n_{sph}, n_{SiO_2} and n_{void} are the refractive indices of the spheres, dense silica and the voids (occupied by air or solvent), respectively. V_{SiO_2} and V_{void} are the fractional volumes in the

spheres occupied by silica and voids, respectively. These can be calculated from the particle density, the density of silica and the density of the substance occupying the pores (air, solvent). Thus, from the Langmuir isotherm, the density and the refractive index of the SiO_2 spheres can be estimated. Assuming the particles have only minor porosity, as the density is slightly higher than that of silica, we estimate their refractive index also to be comparable to that of fused silica ($n = 1.46$).[31,32]

When the spheres are spread at the air–water surface, some of the SDS molecules will be adsorbed onto the ammonium-modified surface by ion exchange, since the hydration energies of Na^+ and Cl^- are higher than those of the organic groups. Thus, the particles are partially hydrophobic. This is supported by the observation that without SDS, particulate films could not be formed. In addition, fully hydrophobised particles (by silylation) only formed weakly ordered structures, as verified by AFM (data not presented). It is likely that, due to the hydrophobic effect, the adsorbed dodecyl sulfate anions will aggregate and one or a few patches of SDS domains will cover the surface of the sphere. Because of their hydrophobicity, these patches will be oriented so as to minimize the contact with the water, *i.e.* upward. The 'uncovered' area of the sphere surface consists of an excess of hydrophilic ammonium chloride groups. Dissociation of the ion pairs creates an electric double layer. Because of the asymmetry of the double layers of the particles, induced by the air–water interface, they act as repulsing dipoles.[34,35] This likely prevents immediate and strong aggregation of the 'floating' spheres and allows them to organise into a close-packed structure as the film is compressed.

We argue that the lattice defects originate, at least in part, from the imperfect monodispersity. Local imperfect hcp matches due to polydispersity accumulate as the particles aggregate into a 2D crystal. This eventually causes a lattice defect (vacancy, 'zippering', *etc.*). Because the mismatch is so large an hcp ordering is not possible. Reducing the polydispersity could significantly improve the ordering quality of the 2D optical crystal.

Optical diffraction properties of the two-dimensional opal

The films show bright colours depending on the direction of illumination and observation. This is caused by the optical Bragg diffraction of the light. Optical Bragg diffraction is physically strongly related to the PBG effect. They are both scattering phenomena of periodic lattices and optical diffraction is often (if not always) observed with PBG materials. In the same way that ordered atomic structures diffract X-rays, structures ordered at the submicron scale diffract visible light.

To characterise the optical properties of the films, optical diffraction spectra were recorded on a spectrofluorimeter in a synchronous scan mode using a home-made mirror accessory. A schematic representation of the experimental setup is shown in Fig. 3. Spectra were recorded while varying the angle θ, and α was set at 45°. A set of spectra obtained in this manner is presented in Fig. 4. As θ is varied from 0 to 45°, the spectra gradually shift from the red to the blue side of the visible spectrum. The maximal intensity of the diffracted light was reached at 460 nm ($\theta = 32°$).

The optical diffraction is envisaged as a Bragg-like reflection on partially virtual sphere planes. This is depicted in Fig. 5. Here, d is the periodic distance between two sphere planes, α is the angle between the incoming wave and the substrate and θ is the observation angle. A path difference between two waves is created as they enter the reverse side of the substrate (x_1) and as they are diffracted by the opal film (x_2). The total path difference between the interfering waves is $x_1 + x_2$.

If positive interference occurs, the waves are transmitted in direction θ, which is manifested as a maximum in the diffraction spectrum. If $x_1 + x_2 = m\lambda$, with m an integer and λ the wavelength of the optical wave, positive interference and thus transmission occurs in the direction of θ. From Fig. 5
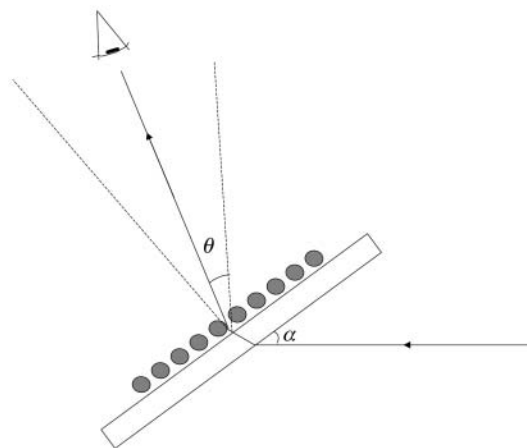

Fig. 3 Schematic representation of the measurement of the optical Bragg diffraction of the SiO_2 films.
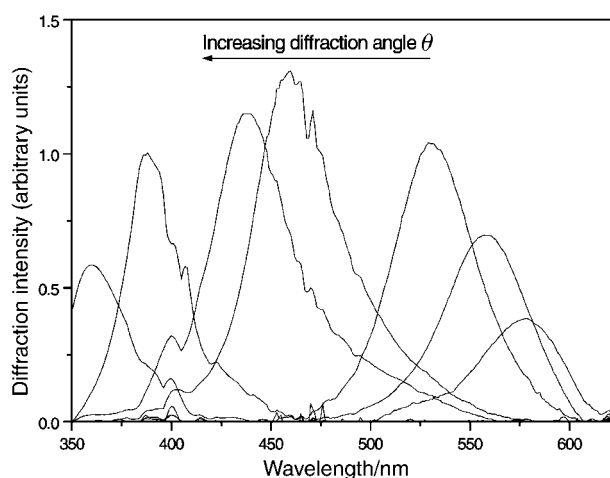

Fig. 4 Optical diffraction spectra of the silica sphere Langmuir–Blodgett film. As θ increases, the spectral positions shift from the red to the blue side of the visible spectrum.
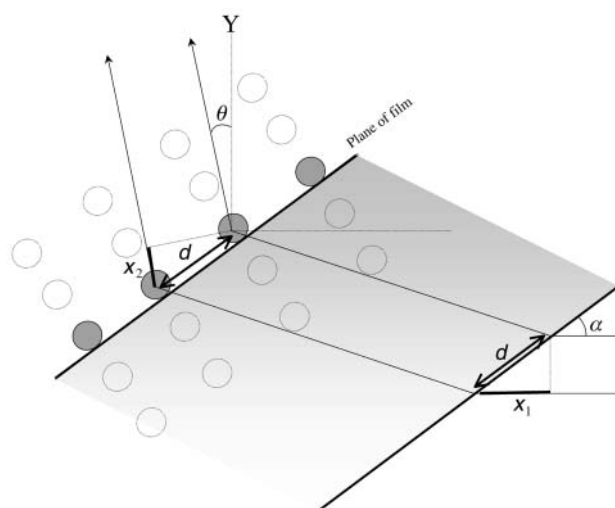

Fig. 5 Schematic representation of the path length difference between two waves diffracted by the SiO_2 structure. The diffraction is envisaged as a Bragg-like reflection on partially virtual sphere planes. The real SiO_2 spheres are shaded and the virtual spheres are dotted. The geometrical parameters are indicated.

$x_1 + x_2$ can be calculated as

$$x_1 + x_2 = d\{\cos\alpha + \sin(\alpha - \theta)\} = m\lambda \tag{3}$$

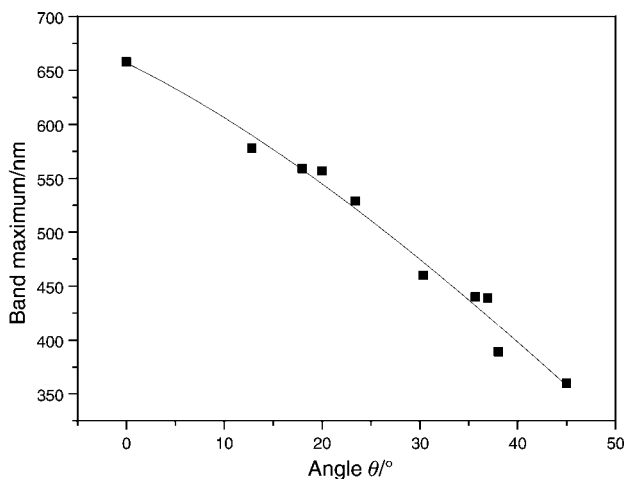in which d is distance between two sphere-planes and the other

Fig. 6 Band maxima of the optical diffraction spectra plotted against observation direction (θ). Eqn. (3) has been fitted to the data to yield a value of 483 nm for the distance, d.

parameters are as indicated in Fig. 5. Eqn. (3) relates the diffraction-band positions to the observation angles (θ). A plot of the band positions *versus* θ for the experimental data is shown in Fig. 6.

Eqn. (3) has been fitted to the data in Fig. 6 to yield a value of 483 nm for the distance, d.

The band positions can be used to determine the lattice constant of the particulate film and thus the particle size. In a two-dimensional hexagonal lattice, the distance (d) is given by

$$\frac{1}{d_{hk}} = \frac{4\left(h^2 + hk + k^2\right)}{3a^2} \qquad (4)$$

in which h and k are Miller indices of the planes and a is the lattice constant.[36] If a is assumed to be 536 nm (as determined by AFM), and $h = 0$ and $k = 1$ (or *vice versa*), then, using eqn. (4), a value of $d_{01} = d_{10} = 464$ nm is obtained. Within the experimental error, the AFM data are in good agreement with the optical diffraction data ($d_{optical} = 483$ nm). Higher Miller indices result in optical diffraction in the UV region for this size of SiO$_2$ spheres. The width of the diffraction bands depends on the quality and the dimensionality of the optical crystal. Reducing the amount of defects and extending the crystal into the third dimension should narrow and intensify the diffraction bands. The focusing of the optical beam generates a spreading of α and also contributes to the bandwidth.

Conclusions

In this report Langmuir–Blodgett deposition has been investigated as a tool for the preparation of large area two-dimensional opal. The Langmuir–Blodgett isotherm has been used to estimate the density and refractive index of the silica spheres. The ordered structure of the opal film allows the measurement of optical diffraction. From these measurements, the particle–particle distance has been estimated. The opal structure was also investigated using atomic force microscopy. The results of the optical diffraction and AFM studies are in good agreement within the experimental error. Although 'true' photonic band gap properties are only exhibited by 3D photonic crystals, 2D materials have been shown to exhibit useful properties. In this respect, we consider Langmuir–Blodgett deposition of 2D opal as a promising route for the preparation of active layers in photonic devices. This requires its integration with other techniques, such as self-assembly of colloidal particles, chemical vapor deposition of highly refractive materials, *etc.*

References

1 A. Ulman, *An Introduction to Ultrathin Organic Films: from Langmuir-Blodgett to Self-Assembly*, Academic Press, Boston, 1991.
2 P. Bertrand, A. Jonas, A. Laschewsky and R. Legras, *Macromol. Rapid Commun.*, 2000, **21**, 319 and references therein.
3 B. van Duffel, C. P. M. Grim, F. C. De Schryver and R. A. Schoonheydt, *Langmuir*, 1999, **15**, 7520.
4 J. Schmitt, G. Decher, W. J. Dressick, S. L. Brandow, R. E. Geer, R. Shashidhar and J. M. Calvert, *Adv. Mater.*, 1997, **9**, 61.
5 B. van Duffel, T. Verbiest, S. Van Elshocht, A. Persoons, F. C. De Schryver and R. A. Schoonheydt, *Langmuir*, 2001, **17**, 1243.
6 H. Fuchs, H. Ohst and W. Prass, *Adv. Mater.*, 1991, **3**, 10.
7 L. S. Li, Z. Hui, Y. Chen, X. T. Zhang, X. Peng, Z. Liu and T. J. Li, *J. Colloid Interface Sci.*, 1997, **192**, 275.
8 Y. Umemura, A. Yamagishi, R. A. Schoonheydt, A. Persoons and F. C. De Schryver, *Langmuir*, 2001, **17**, 449.
9 D. J. Robinson and J. C. Earnshaw, *Langmuir*, 1993, **9**, 1436.
10 K. U. Fulda and B. Tieke, *Adv. Mater.*, 1994, **6**, 288.
11 S. John, *Phys. Rev. Lett.*, 1987, **58**, 2486.
12 E. Yablonovitch, *Phys. Rev. Lett.*, 1987, **58**, 2059.
13 K. Busch and S. John, *Phys. Rev. E*, 1998, **58**, 3896.
14 U. Grüning, V. Lehmann and C. M. Engelhardt, *Appl. Phys. Lett.*, 1995, **66**, 3254.
15 H. Benisty, *J. Appl. Phys.*, 1996, **79**, 7483.
16 V. Berger, *Opt. Mater.*, 1999, **11**, 131.
17 O. Painter, R. K. Lee, A. Scherer, A. Yariv, J. D. O'Brien, P. D. Dapkus and I. Kim, *Science*, 1999, **284**, 1819.
18 S. G. Romanov, T. Maka, C. M. Sotomayor Torres, M. Müller and R. Zentel, *Appl. Phys. Lett.*, 1999, **75**, 1057.
19 Q. Li, C. T. Chan, K. M. Ho and C. M. Soukoulis, *Phys. Rev. B*, 1996, **53**, 15577.
20 M. Scalora, M. J. Bloemer, A. S. Manka, J. P. Dowling, C. M. Bowden, R. Viswanathan and J. W. Haus, *Phys. Rev. A*, 1997, **56**, 3166.
21 V. N. Bogomolov, S. V. Gaponenko, I. N. Germanenko, A. M. Kapitonov, E. P. Petrov, N. V. Gaponenko, A. V. Prokofiev, A. N. Ponyavina, N. I. Silvanovich and S. M. Samoilovich, *Phys. Rev. E*, 1997, **55**, 7619.
22 Y. N. Xia, B. Gates, Y. D. Yin and Y. Lu, *Adv. Mater.*, 2000, **12**, 693.
23 S. G. Romanov, A. V. Fokin and R. M. De La Rue, *J. Phys.: Condens. Mater.*, 1999, **11**, 3593.
24 Y. A. Vlasov, V. N. Astratov, A. V. Baryshev, A. A. Kaplyanskii, O. Z. Karimov and M. F. Limonov, *Phys. Rev. E*, 2000, **61**, 5784.
25 A. van Blaaderen, *MRS Bull.*, 1998, **23**, 39.
26 C. Kittel, *Introduction to Solid State Physics*, John Wiley & Sons, New York, 1976.
27 W. Stöber, A. Fink and E. Bohn, *J. Colloid Interface Sci.*, 1968, **26**, 62.
28 A. K. van Helden, J. W. Jansen and A. Vrij, *J. Colloid Interface Sci.*, 1980, **81**, 354.
29 C. S. Kee, J. E. Kim and H. Y. Park, *Phys. Rev. E*, 1997, **56**, R6291.
30 A. Ayral, J. Phallipou and T. Woignier, *J. Mater. Chem.*, 1992, **2**, 1166.
31 C. J. Brinker and G. W. Sherer, *Sol-Gel Science: the Physics and Chemistry of Sol-Gel Processing*, Academic Press, San Diego, CA, 1990.
32 A. Brunet-Bruneau, S. Fissou, G. Vuye and J. Rivory, *J. Appl. Phys.*, 2000, **87**, 7303.
33 F. L. Pedrotti and L. S. Pedrotti, *Introduction to Optics*, Prentice Hall, Englewood Cliffs, NJ, 1996.
34 P. Pieranski, *Phys. Rev. Lett.*, 1980, **45**, 569.
35 A. J. Hurd, *J. Phys. A: Math. Gen.*, 1985, **18**, L1055.
36 J. M. Schultz, *Diffraction for Materials Scientists*, Prentice Hall, Englewood Cliffs, NJ, 1982.